

Monte Carlo Simulation of the Transport Phenomena in Degenerate Hg_{0.8}Cd_{0.2}Te

N. Dahbi, M. Daoudi, A. Belghachi

Abstract—The present work deals with the calculation of transport properties of Hg_{0.8}Cd_{0.2}Te (MCT) semiconductor in degenerate case. Due to their energy-band structure, this material becomes degenerate at moderate doping densities, which are around 10^{15} cm^{-3} , so that the usual Maxwell-Boltzmann approximation is inaccurate in the determination of transport parameters. This problem is faced by using Fermi-Dirac (F-D) statistics, and the non-parabolic behavior of the bands may be approximated by the Kane model. The Monte Carlo (MC) simulation is used here to determinate transport parameters: drift velocity, mean energy and drift mobility versus electric field and the doped densities. The obtained results are in good agreement with those extracted from literature.

Keywords—degeneracy case, Hg_{0.8}Cd_{0.2}Te semiconductor, Monte Carlo simulation, transport parameters.

I. INTRODUCTION

MERCURY Cadmium Tellurium (MCT-HgCdTe) has been proposed as a material with favorable properties for use in infrared photo-detectors, which represent a physical process with huge number of applications: night vision, civilian and medical imaging, etc. This refers to the properties of this semiconductor, i.e., small band gap, small electron effective mass, large non parabolic conduction band. The majority of MCT- based devices contain a cadmium fraction of $x=0.2$ which at temperature of 77 K allows the photo-detection of the 8-14 μm atmospheric window wavelengths. At this temperature MCT has a narrow band gap; it is about 0.1 eV, so it is easy to become degenerate from small electron densities. This latter feature is important in highly doped regions of infrared photo-detector where all the Coulombic scattering mechanisms are effectively screened and, furthermore, all scattering processes are depending directly on the position of the Fermi level [1]. The need for accurate characterization of MCT in degenerate case brought an enormous number of simulation methods. The most accurate kinetic description is given by the Monte Carlo (MC) method, because it can take into account explicitly both the energy band- structure and various scattering mechanisms of the studied material. The purposes of this work are to use a precise approximation in order to calculate the Fermi level in a degenerate Hg_{0.8}Cd_{0.2}Te at 77 K with different doping

concentration and as result to show the change in material parameters as the gap energy, effective mass and non parabolic factor. The Monte Carlo (MC) simulation is performed in this work in order to calculate the transport parameters in Hg_{0.8}Cd_{0.2}Te as drift velocity, mean energy and drift mobility for degenerate case at 77 K. Hence, we developed our own model which can be easily used for our specific case.

II. FERMI ENERGY IN DEGENERACY CASE

Many of interest situation in semiconductor devices involve high concentrations of electrons, where degeneracy is expected to play an important role. HgCdTe material has a strong non-parabolicity factor ($\alpha=11.4 \text{ eV}^{-1}$) and a narrow band gap, due to this, the degeneracy effects in MCT at 77 K occurs for relatively small electron density ($n > 10^{15} \text{ cm}^{-3}$) [2]. Hence in this case, it is desirable to have an approximation of the Fermi integral in order to relate the Fermi energy by the carrier concentration in non-parabolic semiconductors [3], [4].

In degenerate semiconductors, all the levels under $E_F - 4K_B T$ are occupied and it is assumed that the energy gap in this case takes the following form [5]:

$$E_g = E_{g0} + (E_F - 4K_B T) \quad (1)$$

Where the non-degenerated energy band gap E_{g0} is a function of both, fraction molar of cadmium x and temperature T , it is given by:

$$E_{g0} = -0.302 + 1.93x - 0.81x^2 + 0.832x^3 + 5.35 \times 10^{-4}(1-2x)T \quad (2)$$

This energy is getting in eV and the temperature T is given in Kelvin; where the reduced Fermi energy $\phi_F = (E_F - E_C)/K_B T$ is obtained from the following expression, which takes into account the electron carrier density n and conduction band non-parabolicity α [6]:

$$\phi_F = \ln\left(\frac{n}{b_0 N_C}\right) + b_1 \left(\frac{n}{N_C}\right)^{a_1} + b_2 \left(\frac{n}{N_C}\right)^{a_2} \quad (3)$$

With:

$$b_0 = 1 + 3.75\alpha + 3.28\alpha - 2.461\alpha^2 \quad (4)$$

$$b_1 = 0.994 - 3.333\alpha \quad (5)$$

N. Dahbi is with the Institute of Exact Sciences, Bechar University; n°417, B  char 08000 Algeria (213-49-81-55-81/91; fax: 213-4-81-52-44; e-mail: algeriose@yahoo.com).

M. Daoudi is with the Institute of Exact Sciences, Bechar University; n°417, B  char 08000 Algeria (213-49-81-55-81/91; fax: 213-4-81-52-44).

A. Belgachi is with the Institute of Exact Sciences, Bechar University; n°417, B  char 08000 Algeria (213-49-81-55-81/91; fax: 213-4-81-52-44).

$$b_2 = -(0.577 - 7.93\alpha + 78.6\alpha^2 - 349\alpha^3) \quad (6)$$

$$a_1 = 0.526 + 0.236 \exp\left(-\frac{\alpha + 0.00211}{0.0279}\right) \quad (7)$$

$$a_2 = 0.624 - 12.8\alpha + 128\alpha^2 - 541\alpha^3 \quad (8)$$

Where N_C is the electron effective density, E_F is the Fermi energy, E_C is the conduction band energy, and K_B is the Boltzmann constant. In the figure 1, we plot the reduced Fermi energy versus n-type doping levels at 77 K, the zero energy is taken at the bottom of the conduction band. We observe that when the doping density increases, the band becomes degenerate (i.e. $E_F - E \geq 0$); It is clear that when the doping density is higher than $2 \times 10^{15} \text{ cm}^{-3}$ the MCT is considered as a degenerate semiconductor.

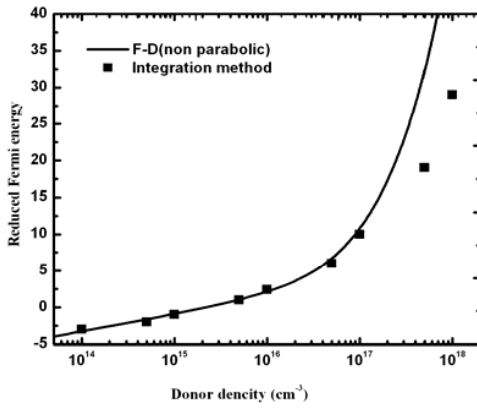


Fig. 1 The reduced Fermi energy as function of donor density.

III. THE BAND STRUCTURE AND DISPERSION RELATION

The atoms in HgCdTe crystallize in zinc-blend structure, this structure treats the conduction band as a combination of the Γ , X and L non-parabolic valleys, which are separate from each other. For this type of semiconductors, it has assumed a simple non-parabolic band structure such that the energy-wave vector relation is given by [7]:

$$E(1 + \alpha^* E) = \hbar^2 k^2 / 2m^* \quad (9)$$

Where: \hbar is the reduced plank constant, k is the wave vector, and m^* is the electron effective mass at the conduction band edge. The non-parabolic factor α^* of the conduction band in degeneracy case is given by:

$$\alpha^* = \frac{1}{E_g} \left(1 - \frac{m^*}{m_0}\right)^2 \left(1 - \frac{E_g \Delta}{3(E_g + \frac{2}{3}\Delta)(E_g + \Delta)}\right) \quad (10)$$

Where m_0 is the free electron mass and $\Delta = 0.9 \text{ eV}$ is the spin split-off energy. The electron effective mass in the narrow band-gap mercury compounds can be established according to the Kane band model, in this work, we use Wiedler's expression [8]:

$$m^* = \frac{1}{-0.6 + 6.333 \left(\frac{2}{E_g} + \frac{1}{E_g + 1} \right)} \quad (11)$$

As result in degenerate HgCdTe, the gap change and become smaller, so the effective mass also, where the non parabolic factor become greater than the case of non degenerate, these changes were modified the transport properties.

IV. MONTE CARLO SILULATION PROCEDURE

In this method, the electron is considered as a point particle, where the motion of the electron inside the crystal subject to electric field and consists in drift and collision processes. In MC algorithm, the trajectory of an electron is followed in both r and k space as sequence of "free-flight-scattering" events. The scattering process responsible for terminating a free flight is determined stochastically using a rejection technique [9]. Usually, the scattering rates are expressed as functions of energy and the self-scattering technique is employed for the selection of time of free flight and scattering mechanisms, the MC algorithm consists of generating random free flight times for each particle, choosing the type of scattering occurring at the end of the free flight, changing the final energy and momentum of the particle after scattering and then repeating the procedure for the next free flight, for more details of the MC model are given in [10].

V. NUMERICAL RESULTS

For the MCT the scattering mechanisms taken into account were: ionized impurity scattering, alloy scattering and polar optical phonon scattering, the inter-valley scattering is negligible in the MCT because the $(\Gamma - L)$ and $(\Gamma - X)$ inter-valley separations energy is being of the order of 2 eV [11]. The analytical expression of each of these collisions is detailed in several works [2], [12]. The scattering rates of MCT as a function of the electron energy for impurity concentration of $n = 5.4 \times 10^{14} \text{ cm}^{-3}$ at $T = 77 \text{ K}$ are reported in figure 2; we observe that at lower energies (below 18 meV) the collisions with the ionized impurities are dominated. However at high energy the total scattering rate increases with energy due to the increasing occurrence of other scattering, polar optical phonon scattering dominates

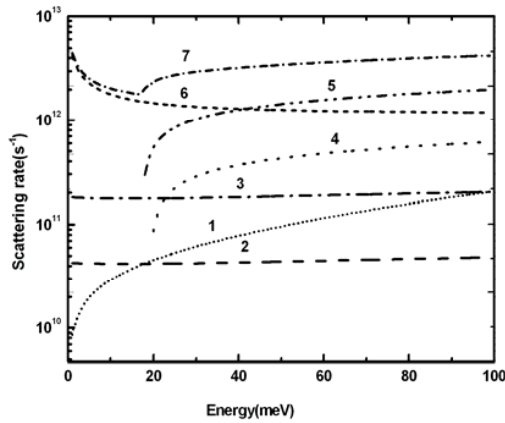


Fig. 2 Scattering events in $\text{Hg}_{0.8}\text{Cd}_{0.2}\text{Te}$ occurring in the simulation as function of energy at 77K. (1) the alloy scattering, (2&3) and (4&5) the optical phonons scattering characteristic of CdTe, HgTe: absorption scattering and emission scattering respectively, (6) ionized impurities scattering and (7) the total scattering

Figure 3 presents the electron drift velocity as a function of electric field for different values of doping densities calculated by our MC simulator in the degenerate case. Simulated results of non-degenerate case as well as experimental results are also reported.

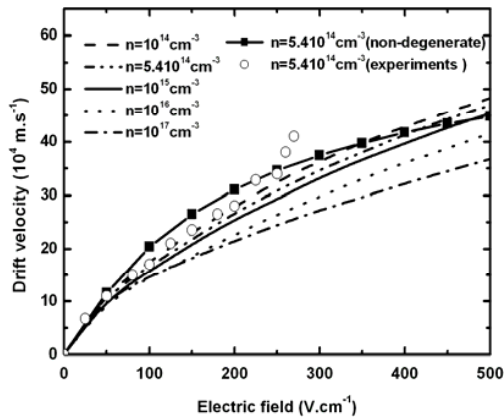


Fig. 3 Drift velocity versus the electric field of $\text{Hg}_{0.8}\text{Cd}_{0.2}\text{Te}$ at 77K, dashed lines are the MC results using the degenerate approximation, line+ symbol obtained in the case of non-degeneracy for $5.4 \times 10^{14} \text{ cm}^{-3}$ and the open circles are the experimental results of Ref. [13].

It is clear that at low electric fields (below 50 V/cm), the drift velocity increases linearly with the electric field as expected in ohmic region. At higher electric fields, the drift velocity increases sub-linearly with the electric field and tends to a saturation value around $5 \times 10^5 \text{ m/s}$. Indeed, in the range of high electric fields, the transport is dominated by collisions with polar phonons; we find also that the electron velocity is higher for lower electron densities. This phenomenon is related to the low electron effective mass and to the relatively

small polar optical phonon energy which allow impurity scattering to be still noticeable when polar optical scattering is important [2]. The experimental drift velocity obtained by Dornhaus [13] for doping concentration of $5.4 \times 10^{14} \text{ cm}^{-3}$ appears to be in a good agreement with the simulated results of degenerate case compared by the drift velocity with the same electron density but without taking into account the degeneracy effect. The improved method reduces the electron velocity by 10%-30% depending on the electric field. Thus the Fermi level approximation and non-parabolicity are essential at high concentration. In figure 4, the variation of the mean energy with the electric field in MCT is reported for impurity density variation between 10^{14} and 10^{17} cm^{-3} . We remark that, for low electric fields the mean energy is practically constant and equal to the thermal equilibrium energy 13 meV; above 50 V/cm the energy increases monotonously with the electric fields.

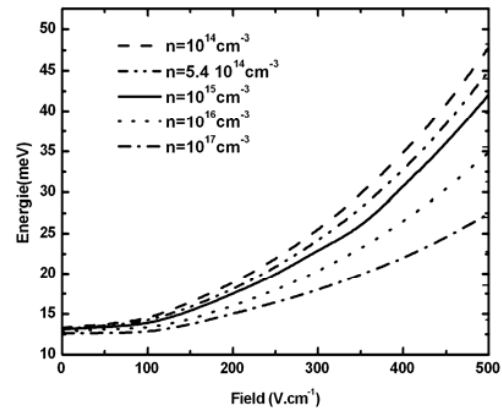


Fig. 4 Energy versus electric field of $\text{Hg}_{0.8}\text{Cd}_{0.2}\text{Te}$ at 77K obtained by Monte Carlo simulation for different values of donor concentration

Another important parameter of the electron transport is investigated here: the drift mobility, figure 5(a) shows Monte Carlo results of the electron drift mobility ($\mu(E) = v(E)/E$) versus electric field; the mobility decreases remarkably for low-electric fields and for the high electric fields it move to saturate below $9 \times 10^4 \text{ cm}^2/\text{Vs}$ for electric field $E = 500 \text{ V/cm}$ with concentration $n = 10^{14} \text{ cm}^{-3}$, so we can confirm that the mobility in the MCT is particularly high.

The doping dependent low-electric field mobility is illustrated in figure 5(b) with the fitting results using the simplified Masetti's formula [14]:

$$\mu(Nd) = \mu_{\min} + \frac{\mu_{\max} - \mu_{\min}}{1 + \left(\frac{Nd}{Cr}\right)^{\beta}} \quad (12)$$

Where Nd is the donor density, where $\beta = 0.90917$,

$Cr = 3.020 \times 10^{15}$ are adjustable parameters, and where $\mu_{\max} = 2.3 \times 10^5 \text{ cm}^2/\text{V.s}$ and $\mu_{\min} = 1.8 \times 10^5 \text{ cm}^2/\text{V.s}$ are the maximum and the minimum drift mobility respectively. It is clear, that the mobility does not vary significantly with the level of donor doping range considered; it decreases with the ionized impurity concentration slowly, so it is important to study high-field transport in the MCT. In general, our results appear to be in a good agreement with those extracted from literature.

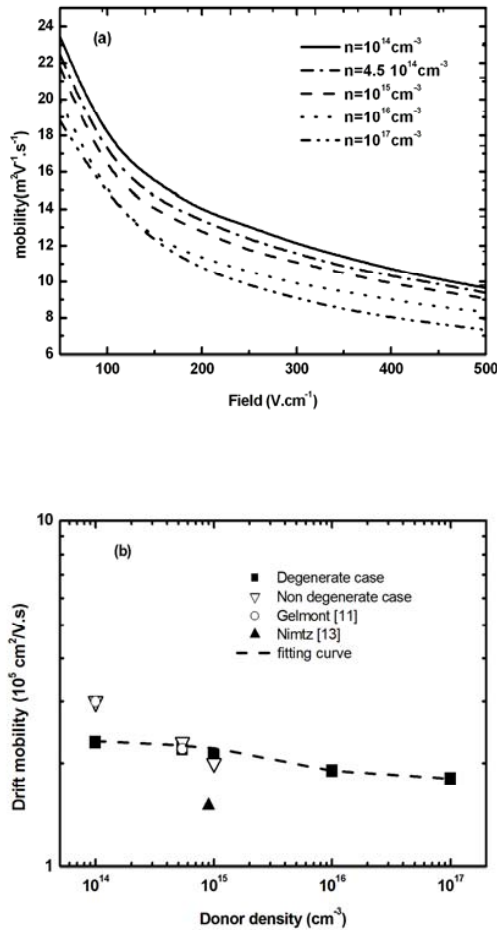


Fig. 5 Electron drift mobility in $\text{Hg}_{0.8}\text{Cd}_{0.2}\text{Te}$ versus; (a) electric field and (b) doping concentration at 77K for two cases: degenerate case (■), non degenerate case (▽), and (---) fitting curve compared with those extracted from literature ○-Ref.[11], and ▲-Ref.[13].

VI. CONCLUSION

We have performed a Monte Carlo study of electron transport in steady-state regime in bulk $\text{Hg}_{0.8}\text{Cd}_{0.2}\text{Te}$ at 77 K, which takes in the consideration both non-parabolic energy band and the degeneracy case. In our work, the effects of the scattering mechanisms on the drift velocity, the mean electron

energy and low field mobility of $\text{Hg}_{0.8}\text{Cd}_{0.2}\text{Te}$ are determined. Our calculations indicate that the drift velocity and the low-field mobility are limited strongly by the ionized impurity scatterings. These results are in reasonable agreement with the reported data. A deeper investigation will enable to calculate also the temperature-dependent mobility.

REFERENCES

- [1] S.D.Yoo, B.G.KO, G.S.Lee, J.G.Park, and K.D.Kwack, *Opto-Electronics Rev.* Vol.7, pp.339-345, 1999.
- [2] C.Palermo, L.Varani, J.C.Vaissière, E.Starikov, P.Shiktorov, V.Gruzinskis, and B.Azaïs, *Solid-State Electronics*, vol.53, pp. 70-78, 2009.
- [3] Z.J.Quan, G.B.Chen, L.Z.Sun, Z.H.Ye, Z.F.Li, and W.Lu, *Infrared Physics and Technology*, vol. 50, pp. 1-8, 2007.
- [4] Sudha Gupta, R.K.Bhan, and V.Dhar, *Infrared Physics and Technology*, vol. 51, pp. 259-262, 2008.
- [5] Z.Djuric, Z.Jaksic, A.Vujanic, and M.Smiljanic, *Infrared Phys.*, vol. 34, pp. 601-605, 1993.
- [6] X.A.Humet, F.S.Mestres, and J. Millan, *J. Appl. Phys.*, vol.54, pp.2850-2851, 1983.
- [7] A.Dutta, P.S.Mallick, and Mukhopadhyay, *Int.J.Electronics*, vol. 84, pp. 203-214, 1998.
- [8] M. H. Weiler, *Semiconductor and Semimetals.*, NewYork: ed. R.Willardson and R.K. Beer, 1981.
- [9] C. Jacoboni, and L. Reggiani, *Mod. Phys.Rev.*, vol. 55, pp. 645-705, 1983.
- [10] M. Akarsu, and Ö. Özbaz, *Mathematical and Computational Applications*, vol. 10, pp. 19-26, 2005.
- [11] B.Gelmont, B.Lund, K.Kim, G.U.Jensen, M.Shur, and T.A.Fjeldly, *J.Appl.Phys.*, vol.71, pp. 4977-4982,1992.
- [12] C.Jacoboni, P.Lugli, *The Monte Carlo Methods for Semiconductor Device Simulation*. Wien: Springer-Verlag, 1989.
- [13] G.Nimtz, R.Dornhaus, and K.H.Muller, *Phys.Rev.B*, vol. 10, pp. 3302-3310, 1974.
- [14] G.Masetti, M.Severi, S.Solmi, *IEEE Trans. Electron Dev.*, vol. ED30, pp.764-769, 1983.

*